Physica A 640 (2024) 129697

Contents lists available at ScienceDirect

Physica A

journal homepage: www.elsevier.com/locate/physa

Cooperative bound states in quantum walks of interacting particles

M.F.V. Oliveira [a], M.S. Santos Junior [a], Michele B. Coêlho [b], F.A.B.F. de Moura [a], W.S. Dias [a,*]

[a] Instituto de Física, Universidade Federal de Alagoas, 57072-900 Maceió, Alagoas, Brazil
[b] Instituto de Física, Universidade Federal do Rio Grande do Sul, 91501-970 Porto Alegre, Brazil

ARTICLE INFO

Keywords:
Quantum walks
Interacting particles
Bound states
Bloch oscillations

ABSTRACT

Although multiparticle quantum walks have been claimed to be universal for quantum computing, fundamental issues still need further understanding, such as the formation of bound states and their role in particle dynamics. By considering the framework of two-particle quantum walks, we study particles with short- or long-range interactions between them and observe the emergence of local and non-local bound states associated with these interactions. We show that such bound states can perform competitive and cooperative influence with existing states, sometimes resulting in unusual dynamics. In addition to revealing the optimal scenarios for particles to perform coherent dynamics, we also show that cooperative scenarios between bound states are responsible for robustly correlated quantum walks. Thus, coherent dynamics of particles can be maintained even for strong interaction strengths, avoiding the nonmonotonic behavior exhibited by systems with only on-site interaction.

1. Introduction

Quantum walks have attracted much attention recently, not only for being a versatile and highly controllable platform for studying quantum systems but also for their promising character of performing quantum computing. Coherent superposition and quantum interference are responsible for different dynamics from their classical analog, well-known for stochastic motion. Understanding the role played by underlying quantum states is one of the key points, which becomes even more challenging when more than one particle is walking simultaneously.

Quantum effects are considerably enhanced when two or more quantum walkers are simultaneously present, such that systems with many interacting quantum walkers have been considered to perform universal and efficient quantum computation [1–3]. However, the Hilbert space describing multiparticle quantum walks grows exponentially with the linear increase in particle number and the lattice size [4]. Thus, studies with low density of particles have been explored, presenting valuable results. The additional power shown by quantum walks of interacting particles for distinguishing nonisomorphic strongly regular graphs is an example [5]. Algorithms based on two interacting particles can distinguish nonisomorphic graphs that non-interacting particles cannot. Such an increase in distinguishing power is associated with spatial correlations and entanglement between particles undergoing the quantum walk [6]. Furthermore, two-particle interacting quantum walks have also been explored for information protection and the development of safer quantum protocols [7].

The weakening of Anderson localization in disordered or aperiodic quantum walks as a function of interaction between particles is another scenario. Initially described by persistent currents in the presence of Coulomb interaction [8,9], this phenomenon is recovered by two particles walking in a disordered lattice [10]. More recent studies unveil the nonmonotonic character of such

* Corresponding author.
E-mail address: wandearley@fis.ufal.br (W.S. Dias).

https://doi.org/10.1016/j.physa.2024.129697
Received 2 December 2023; Received in revised form 28 February 2024
Available online 18 March 2024

weakening [11,12], in agreement with results reported for multiparticle systems [13–17]. A decrease in the degree of localization has also been reported in quantum walks assisted by particle-number changes [18]. Such number-changing interactions still decrease mixing and hitting times on binary trees, a structure of interest in quantum computing [19,20].

An essential prerequisite for validation and realization of high-fidelity quantum information processing, experimental control over the dynamics of quantum multi-particle systems has recently been demonstrated. Two-particle quantum walks were initially implemented on an integrated waveguide architecture within a discrete-time framework, which explored the quantum dynamics of noninteracting bosonic or fermionic particles [21]. Bosonic atoms in an optical lattice were used to implement two-particle quantum walks with tunable interactions [22]. As a result, it was reported that particles can form a stable repulsively bound pair with effective single-particle behavior and perform Bloch oscillations with a specific frequency. Analogous results have been experimentally achieved with photons in a waveguide array [23] and designed electric circuits [24], demonstrating the possibility of accessing and controlling quantum states across different frameworks. This behavior, characterized by twice the fundamental frequency, corroborates the theoretical prediction in Ref. [25]. Such bound pair of particles behaving as a molecule has been shown either by considering discrete-time quantum walks [26] as for a Thirring walk, a quantum walk based on the two-particle sector of a quantum cellular automata [27,28].

More recent studies have explored quantum walks with three or more particles. Larger clusters of interacting particles can exhibit fractional Bloch oscillations, with frequencies proportional to the number of particles clustered in a bound state [29]. Quantum walks of interacting indistinguishable particles point out three-boson bound states as an ideal metrological state for the precision measurement of gravitational force [30]. Studies considering different particles on the walk have reported the formation of intercomponent bound states [31] and quantum correlations between noninteracting particles mediated by an additional third particle [32].

Despite notable advancements [33–35], there remains a need for a deeper understanding of quantum walks involving interacting particles. Exploring the formation of bound states comprising multiple particles and their effects on particle behavior holds the potential to establish specific quantum logical correlations and operations that might otherwise be unattainable. Furthermore, this research subject is closely intertwined with crucial physics and quantum technology elements, including an in-depth survey of fundamental quantum properties such as entanglement and superposition, advancing more efficient quantum circuits, and optimizing quantum computing at the hardware level. Our objective here is to investigate whether nonlocal interactions between particles are responsible for the emergence of different bound states and to examine the behavior of particles in the presence of multiple coexisting bound states. To address such questions, we consider the well-established extended Hubbard model [36] over a theoretical framework of two-interacting particle quantum walks. Numerical analysis shows the emergence of different bound states as we consider the particles interacting at a distance. Our findings advance the understanding of the interplay between available states in a quantum walk, unveiling the existence of cooperative aspects between bound states and competitive regimes between existing states. As a consequence, unusual quantum correlations are established. We report that cooperative scenarios between bound states can promote robustly correlated quantum walks, where coherent dynamics are maintained even for strong interaction strengths. Optimal scenarios for achieving such coherent dynamics in different interparticle interaction ranges are shown.

2. Model and formalism

Quantum walks have been fundamental in exploring complex quantum systems, offering a powerful tool for quantum simulation and algorithms [37–40]. Both frameworks, discrete- and continuous-time, have allowed for modeling a wide range of physical phenomena and addressing advanced computational challenges. Introduced by Aharonov et al. [41], discrete-time quantum walks design the walker advancing through discrete steps dictated by a dynamic internal degree of freedom, effectively performing as a quantum coin. While recognizing the significant results for two-interacting particles in discrete-time quantum walks [26–28], we consider continuous-time quantum walks, whose connection with their classical counterpart is established based on the analogy between the quantum mechanical Hamiltonian and the classical transfer matrix [42]. Thus, the walker hops to adjacent nodes on a graph following the time-dependent Schrödinger equation.

The problem involves analyzing the quantum walk of two interacting particles in one-dimensional lattices with N sites. As a step towards understanding the effect of nonlocal interactions on such systems, we consider an extended version of the Hubbard model that considers particles with nearest-neighbor interaction in addition to on-site interaction [36]. The following Hamiltonian describes the system

$$\begin{aligned} H &= \sum_{n,\alpha=a,b} [J(\hat{b}^{\dagger}_{n+1,\alpha}\hat{b}_{n,\alpha} + \hat{b}^{\dagger}_{n,\alpha}\hat{b}_{n+1,\alpha}) + Fnd\hat{\eta}_{n,\alpha}] \\ &+ \sum_{n} [U(\hat{\eta}_{n,a}\hat{\eta}_{n,b}) + V(\hat{\eta}_{n,a}\hat{\eta}_{n+1,b} + \hat{\eta}_{n+1,a}\hat{\eta}_{n,b})]. \end{aligned} \tag{1}$$

Here, $\hat{b}_{n,\alpha}(\hat{b}^{\dagger}_{n,\alpha})$ is the annihilation (creation) operator of particle α [$\alpha \in (a,b)$] at site n. $\hat{\eta} = b^{\dagger}_{n,\alpha}b_{n,\alpha}$ is the corresponding particle number operator and J is the single-particle tunneling amplitude between neighboring sites. The on-site and nearest-neighbor interactions between two distinguishable bosons (or fermions with opposite spins) are denoted by U and V, respectively. d is the lattice spacing and F is the constant force. By introducing an external force, we can utilize well-established outcomes as a benchmark, as the specific frequency of Bloch oscillations serves as a distinctive signature of correlated particle motion resulting from forming bound states between them [25]. An experimental setup can be achieved and precisely controlled by employing ultracold atoms trapped in a sufficiently deep lattice potential [22,43]. The hopping and interaction terms depend on the depth of

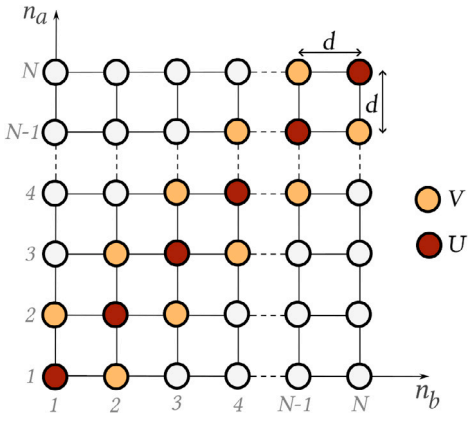

Fig. 1. A quantum-walk graph corresponding to two-interacting particles described by Hamiltonian in Eq. (1). Two discrete indices (n_a, n_b) identify each node representing the basis states $|n_a, n_b\rangle$. Nodes on the main $(n_a = n_b)$ and nearest-neighbor $(n_a = n_b \pm 1)$ diagonals account for on-site (U) and nearest-neighbor (V) interaction between particles, respectively.

the optical lattice potential and the Feshbach resonance framework, with a lattice tilt providing the necessary F. Recent progress in electrical circuits [24] and superconducting processors [44,45] also positions them as promising experimental frameworks.

A corresponding quantum-walk model visualizes state transitions in a quantum system as a network of interconnected nodes. The Hamiltonian outlined in Eq. (1) can be mapped by depicting the different states as nodes on a graph, as shown in Fig. 1. In this context, the lattice sites correspond to positions $(n_a, n_b) = (jd, kd)$, where j, k are elements of the sets $[1, N]$ and $\mathbb{N}^*$. One assumes that the states representing the nodes $|n_a, n_b\rangle = |n_a\rangle \otimes |n_b\rangle$ span the whole accessible Hilbert space $\mathcal{H} = \mathcal{H}_{n_a} \otimes \mathcal{H}_{n_b}$. Here, $\mathcal{H}_{n_a}$ and $\mathcal{H}_{n_b}$ represent the respective Hilbert spaces of particles a and b. The resulting size of the graph is therefore $N^2 = N \times N = dim(\mathcal{H})$. Highlighted nodes on the main $(n_a = n_b)$ and nearest-neighbor $(n_a = n_b \pm 1)$ diagonals account for on-site (U) and nearest-neighbor (V) interaction between particles, respectively.

By considering f_{n_a,n_b} the amplitude probability of finding the particle a at site n_a and the particle b at site n_b of the lattice, we expand the normalized state vector of the system $|\psi(t)\rangle$ in the Wannier representation

$$|\psi(t)\rangle = \sum_{n_a,n_b} f_{n_a,n_b}(t)|n_a, n_b\rangle, \tag{2}$$

The evolution equations for the amplitudes f_{n_a,n_b}, obtained from the time-dependent Schrödinger equation, are solved numerically using a high-order method based on the Taylor expansion of the evolution operator [25]. Thus, the state vector at a time t is given by applying the unitary transformation $|\psi(\Delta t)\rangle = \Gamma(\Delta t)|\psi(t = 0)\rangle$ recursively, where

$$\Gamma(\Delta t) = e^{-iH\Delta t/\hbar} = 1 + \sum_{l=1}^{l_f} \frac{(-iH\Delta t/\hbar)^l}{l!}, \tag{3}$$

is the quantum mechanical time evolution operator. The following results were taken by using $\Delta t = 0.05$, and $l_f = 20$. This cutoff was sufficient to keep the wave function norm conservation $(|1 - \sum_{n_a,n_b} |\psi_{n_a,n_b}|^2| \leq 10^{-15})$ along the entire time interval considered. Furthermore, we use dimensionless units $F/J, U/J, V/J$, and set $\hbar = J = d = 1$.

Since the absence of net displacement of the wave-packet centroid is achieved for an initial Fock state with the particles occupying a single site [46,47], we consider an initial Gaussian wave packet with width σ

$$\langle n_a, n_b|\psi(t = 0)\rangle = \frac{1}{A} e^{-[(n_a - n_a^0)^2 + (n_b - n_b^0)]/4\sigma^2}, \tag{4}$$

centered at the initial positions (n_a^0, n_b^0), with $n_a^0 = N/2$ and $n_b^0 = N/2$. A is a normalization factor. Preliminary studies have indicated no notable variations when investigating system sizes ranging from $N = 100$ to $N = 250$. To maintain wave function norm conservation and mitigate edge effects within a viable computational effort, we have opted for lattices with $N = 150$ for the subsequent analysis. Through the above-described protocol, we computed typical quantities that can bring information about particle dynamics, as will be detailed below.

3. Results

We start following the time evolution of the wave-packet centroid associated with each particle, defined as

$$\overline{n}_i(t) = \sum_{n_a,n_b} n_i |f_{n_a,n_b}(t)|^2, \qquad i = a, b \tag{5}$$

Due to the symmetry of the initial state and interaction Hamiltonian, one has that $\overline{n}_a(t) = \overline{n}_b(t)$. Using a lattice with $N = 150$ sites, $\sigma = 1$, and $F = 0.5$, we investigated the influence of non-local interaction by evaluating different interaction strengths between

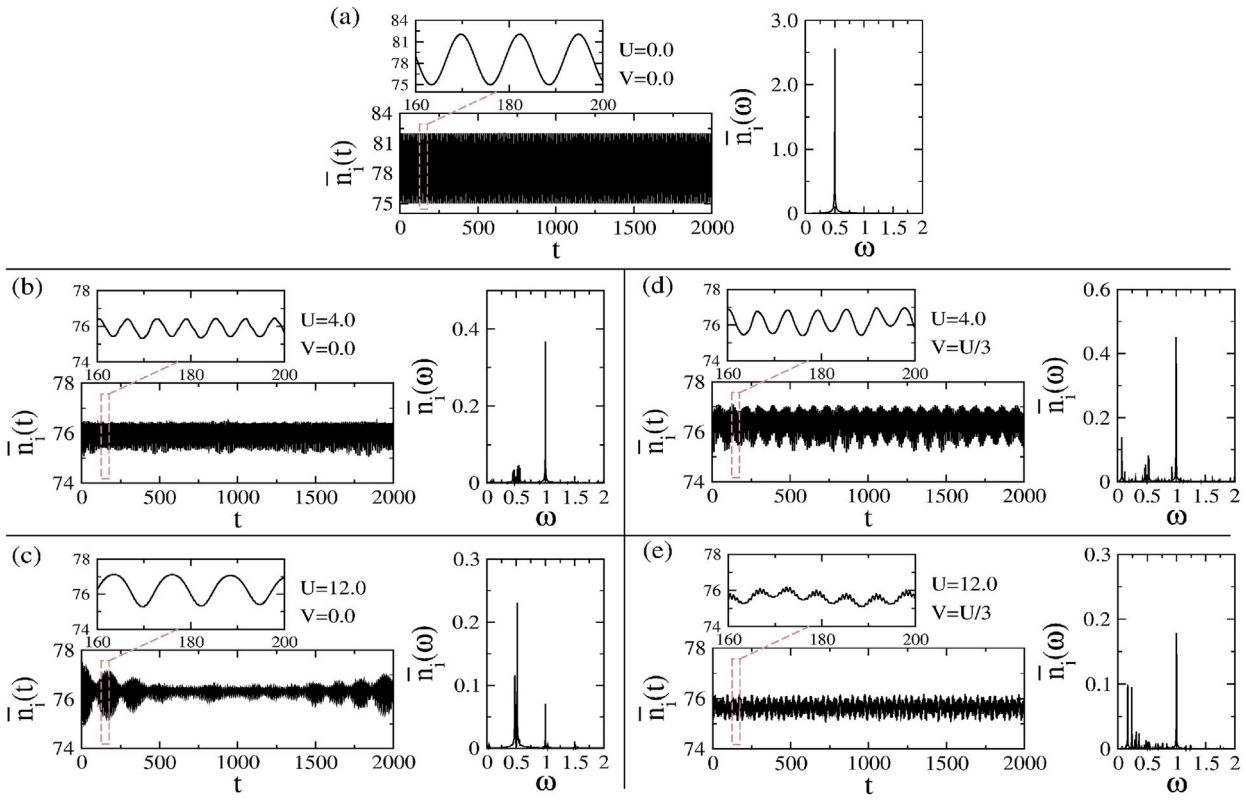

Fig. 2. Time-evolution of wave-packet centroid and the respective Fourier transform for systems with distinct interaction strength between particles: (a) $U = 0$ and $V = 0$; (b) $U = 4$ and $V = 0$; (c) $U = 12$ and $V = 0$; (d) $U = 4$ and $V = U/3$ and (e) $U = 12$ and $V = U/3$. The oscillatory pattern developed by systems with on-site and nearest-neighbor interactions shows a predominant scenario of coherent hopping even for strong interaction strength, differing from the behavior exhibited by systems with only on-site interactions.

particles. Here, we consider a nearest-neighbor interaction to mimic a screening of the Coulomb interaction by orbitals, known to decrease with distance [48]. Thus, we focus on $V = U/3$ without loss of generality for $V < U$. To evaluate the contribution arising from this non-local interaction, we use as reference the case with only on-site interaction ($V = 0.0$) [25]. Such a scenario is shown in Fig. 2a-c for $U = 0.0, 4.0, 12.0$, respectively. We observe all centroids exhibiting an oscillatory pattern consistent with Bloch oscillations. For $U = 0.0$, the system is composed of non-interacting particles. The respective Fourier transform [panel with $\overline{n}_I(\omega)$] clearly shows a predominant oscillation frequency ($\omega = F$) consistent with particles performing independent hopping [49,50]. An oscillatory pattern with a dominant frequency close to $\omega = 2F$ is achieved for $U = 4.0$, which corroborates the scenario of particles hopping coherently [22,23,25]. The wave-packet component corresponding to bound states exhibits signatures of dynamical evolution typical of a single particle composed of the particles pair. The effective local potential felt by this composed particle is proportional to $2Fnd$, thus explaining the observed frequency doubling ($\omega = 2F$). However, the $\omega = F$ frequency is reamplified and becomes predominant for strong enough interactions (here $U = 12.0$). This nonmonotonic behavior demonstrates the competitive character between the existing bound and unbound states. As the interaction increases further, the high energy cost for double occupancy renders coherent particle hopping increasingly unfavorable. Thus, the independent hopping of particles (signaled by the frequency $\omega = F$) becomes predominant over the coherent hopping (signaled by the frequency $\omega = 2F$). In Fig. 2d–e, we examine a system with particles subject to on-site and nearest-neighbor interactions under the same settings as the previous reference scenario. Differing from the reference scenario, we observe a predominant oscillatory pattern with a frequency close to $\omega = 2F$ for both $U = 4.0$ and $U = 12.0$. Considering the emergence of nearest-neighbor bound states due to nearest-neighbor interaction [51], this behavior suggests a cooperative interaction between the different existing bound states, contributing to the predominantly coherent hopping of particles even when they are under strong interaction strengths.

To understand the role played by the nearest-neighbor interaction in sustaining the coherent particle hopping for strong interactions, we explored the long-time average of the double occupancy probability ($\overline{\text{DOP}}$), probability of occupying neighboring sites ($\overline{\text{NOP}}$), and next-nearest-neighboring occupancy probability ($\overline{\text{NNOP}}$). These quantities are computed by using the same lattice size of $N = 150$ sites, $\sigma = 1$, and $F = 0.5$ employed before. In Fig. 3, we show such occupancy probabilities as a function of U, both for $V = 0.0$ and $V = U/3$. Although the particles exhibit independent hopping in the absence of interaction, the external force makes them remain trapped over a finite segment. Thus, we observe non-null values of occupancy probabilities even in the absence of particle–particle interactions. As the interaction is turned on, correlated dynamics of particles are observed. The $\overline{\text{DOP}}$ growth

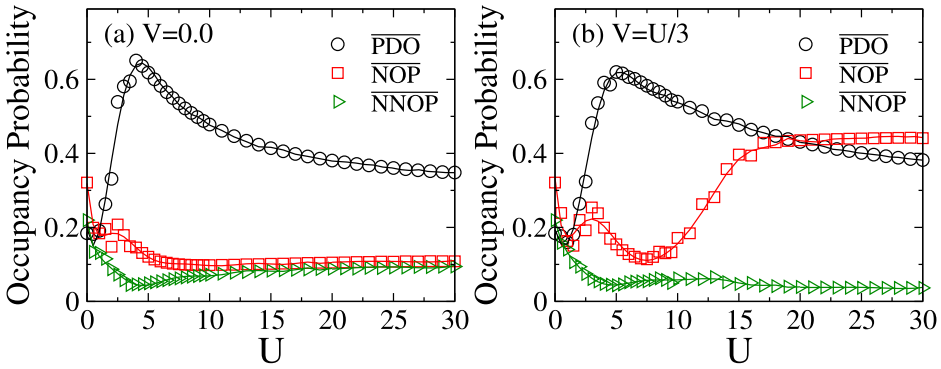

Fig. 3. The time average of occupancy probability versus on-site interaction strength U for quantum walks in which particles present (a) only on-site interaction and (b) on-site and nearest-neighbor interaction. The competitive character between bound and unbound states is responsible for an optimal scenario for the coherent dynamics of particles occupying the same site around $U = 4$. Such coherent hopping is supported for strong U by the emergence of nearest-neighbor bound states, now with particles occupying neighboring sites.

shows the particles predominantly occupying the same site. However, we observe a nonmonotonic behavior in such a correlated dynamic as U increases even more. Such behavior is associated with the emergence of on-site bound states and the competitive effects between them and the unbound states. The first ones, which favor coherent hopping, cover the energy range $U \leq E \leq \sqrt{16+U^2}$ for systems with only on-site interaction and $U \leq E \leq V + \sqrt{16+(U-V)^2}$ for systems with on-site and nearest-neighbor interaction between particles [25,51]. The others cover the energy range $-4 \leq E \leq 4$ and correspond to the states of uncorrelated particles. The emergence of U favors the influence of bound states on particle dynamics as the interaction increases. However, the sub-band of bound states separates and moves away from the band of unbound states as the interaction becomes very strong [52]. This scenario favors the predominance of unbound states over particle dynamics. As a result, optimal coherent dynamics are achieved with intermediate interaction strength, leading to Bloch oscillations with both particles predominantly occupying the same sites. This occurrence corresponds to the disentanglement between bound and unbound state sub-bands.

While the described scenario elucidates the reamplification of independent oscillations ($\omega = F$) for strong interactions, as depicted in Fig. 2c, the behavior of systems with both on-site and nearest-neighbor interactions requires explanation. In Fig. 3b, we observe a slower decrease of $\overline{\text{DOP}}$ and the upward trend of $\overline{\text{NOP}}$ under strong particle–particle interactions. The first observation occurs because of the widening of bound states sub-band in the function of V [51]. The second one is consistent with the emergence of nearest-neighbor states covering the range $V \leq E \leq V + 4/V$ [51]. These states are responsible for a coherent dynamic in which particles occupy neighboring sites. As with on-site bound states, a competitive character promotes the relevance of these states when they are close to detaching from the main band. Such behavior consolidates a cooperative effect between on-site and nearest-neighbor bound states, which favors the maintenance of a coherent dynamic of particles signaled by predominant frequency $\omega = 2F$ for strong interactions in Fig. 2e.

As an additional analysis, we explore in Fig. 4 quantum walks in which the on-site interaction is negligible ($U = 0$) and particles interact only when they are on neighboring sites. Such a system is consistent with Ref. [30] and can be implemented with the current technology of ultracold atoms [22,53]. Fig. 4 shows centroids and the respective Fourier transforms for (a) $V = 4$ and (b) $V = 12$, considering the same lattice size of $N = 150$ sites, $\sigma = 1$, and $F = 0.5$ employed before. We observe coherent Bloch-oscillating quantum walks, signaled by the predominant frequency $\omega = 2F$. Thus, it becomes evident that non-local bound states promote coherent hopping of particles. Unlike the systems where the particles have only on-site interaction, now we observe particles predominantly occupying nearest-neighbor sites. Such an aspect is shown by the behavior of $\overline{\text{NOP}}$ in Fig. 4c. We also note the coherent dynamics (frequency doubling) predominating even for strong interaction strengths (here $V = 12$). This scenario is consistent with a higher coherent hopping probability and a slower decay as the interaction between particles is strengthened (compare Fig. 2a to Fig. 4c). Despite this difference, the competitive character between bound and unbound states is still observed, present in the nonmonotonic behavior of $\overline{\text{NOP}}$ and the lower amplitude modes in $\overline{\text{n}}_i(\omega)$.

Going beyond the scenario with on-site and nearest-neighbor interactions, we investigated the quantum walks with long-range interaction between particles. The following Hamiltonian describes the system:

$$H = \sum_{n,\alpha=a,b} [J(\hat{b}^{\dagger}_{n+1,\alpha}\hat{b}_{n,\alpha} + \hat{b}^{\dagger}_{n,\alpha}\hat{b}_{n+1,\alpha}) + Fnd\hat{\eta}_{n,\alpha}] + \sum_{n_a,n_b} Ue^{-|n_a-n_b|/\xi}\hat{\eta}_{n,a}\hat{\eta}_{n,b}. \quad (6)$$

Just like before, $\hat{b}_{n,\alpha}(\hat{b}^{\dagger}_{n,\alpha})$ is the bosonic annihilation (creation) operator at site n of two distinguishable particles [$\alpha \in (a,b)$], and $\hat{\eta} = b^{\dagger}_{n,\alpha}b_{n,\alpha}$ is the corresponding particle number operator. J denotes the single-particle tunneling amplitude between neighboring sites. U is the strength of the particle–particle interaction at a given site n when both occupy the same position. This strength decays exponentially with the distance between the particles $|n_a - n_b|$.

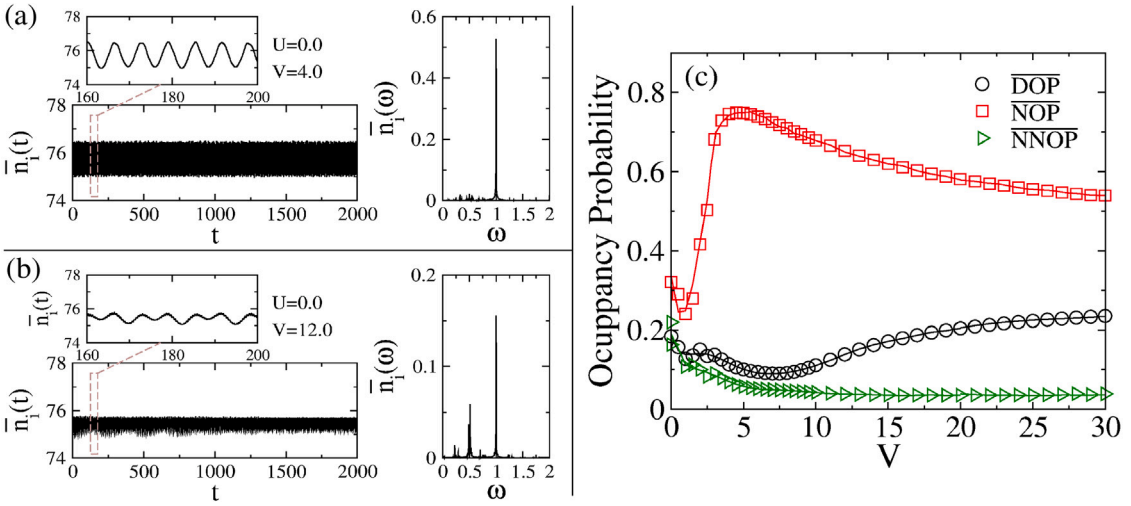

Fig. 4. (a–b) Time-evolution of wave-packet centroid and the respective Fourier transform for quantum walks in which particles present only nearest-neighbor interaction show coherent hopping of particles achieved by the nearest-neighbor bound states. (c) The time average of occupancy probability versus nearest-neighbor interaction strength V unveils that such coherent dynamics are dominated by particles occupying neighboring sites.

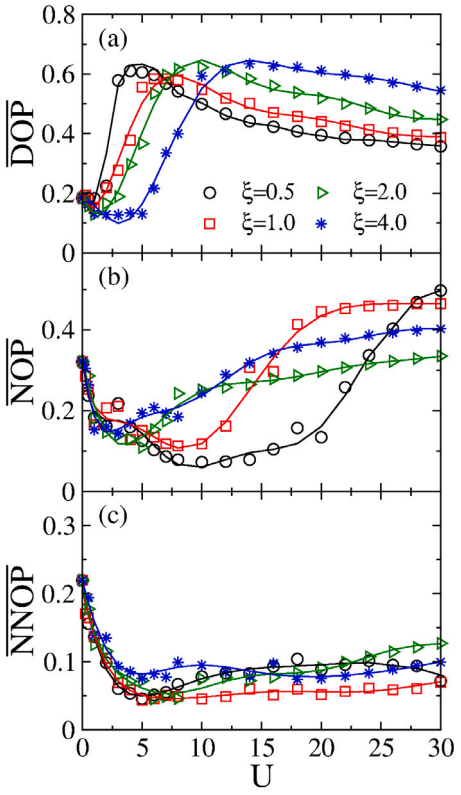

Fig. 5. The time average of (a) double occupancy probability, (b) probability of occupying neighboring sites, and (c) next-nearest-neighboring occupancy probability computed for different U strengths and interaction range ξ. The optimal U interaction strength for displaying double occupancy probability increases as ξ increases, while the ascendance of occupation probability at neighboring sites arises for smaller and smaller interactions. Such behavior signals changes in the cooperative character between the bound states as we increase the interaction strength.

Employing the identical formalism and parameter sets previously applied for the time evolution, we probe the influence of the interaction range ξ on the Bloch-oscillating dynamics of two particles. We keep the lattice size, initial wave-packet width, and F the same as Figs. 2–4 and compute the occupancy probabilities $\overline{\text{DOP}}$, $\overline{\text{NOP}}$, $\overline{\text{NNOP}}$ in the function of interaction strength U. We

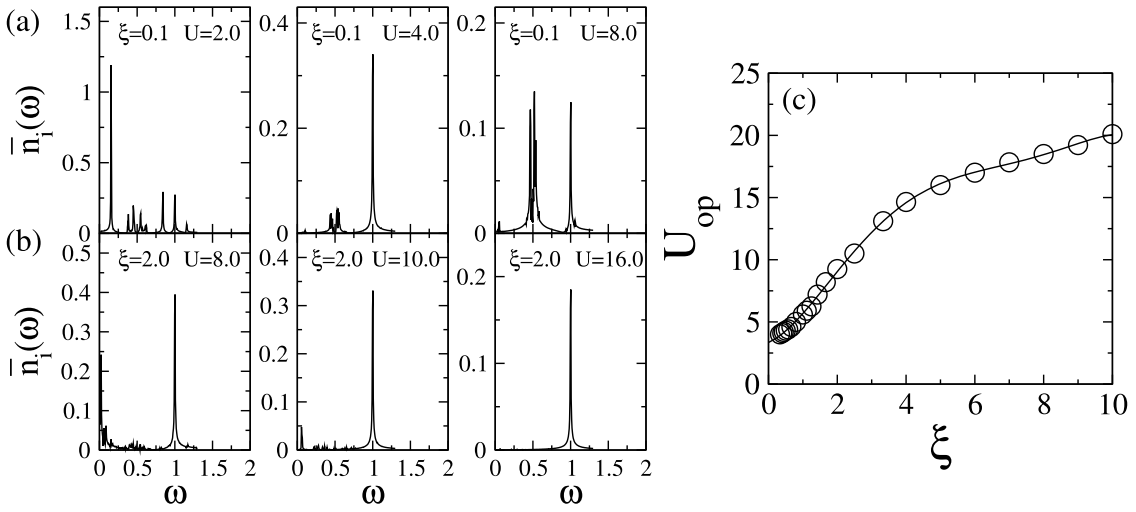

Fig. 6. (a-b) Fourier transform obtained from the time-evolution of wavepacket centroid. (a) For small ξ, competition between bound and unbound states makes the coherent hopping of particles perform better for intermediate interaction strength. (b) As ξ increases, the coherent hopping in which particles occupy neighboring sites also influences the dynamics of particles. Such a cooperative effect of bound states dominates the particle dynamics even for strong interactions. (c) Optimal interaction strength for coherent particle dynamics increases with ξ.

start by exploring the change in the interaction range $\xi = 0.5, 1.0, 2.0, 4.0$. In Fig. 5a we observe a slower decaying rate of $\overline{\text{DOP}}$ as the interaction range increases. Furthermore, the optimal U interaction strength for displaying double occupancy probability increases as ξ increases. On the other hand, the ascendance of occupation probability at neighboring sites ($\overline{\text{NOP}}$) arises for smaller and smaller interaction strengths as we increase the interaction range ξ. As double occupancy and nearest-neighbor occupancy were more energetically favorable, $\overline{\text{NNOP}}$ remains much less sensitive to interaction range ξ than the $\overline{\text{DOP}}$ and $\overline{\text{NOP}}$.

Optimal coupling signals the best scenario of particles moving coherently, with the least influence of unbound states or competitive effects. Such features are studied in Fig. 6a-b, where we present the Fourier transform obtained from the time evolution of the centroid for configurations around the interaction of optimal coupling. For small enough ξ, the system behaves as if it has only on-site interaction. We observe a nonmonotonic character in the coherent hopping of the particles. The competition between bound and unbound states previously reported makes such coherent dynamics of particles perform better for intermediate interaction strength. As ξ increases, this nonmonotonic behavior is no longer observed. With the emergence of non-local bound states, the coherent hopping in which particles occupy neighboring sites also influences the dynamics of particles. Fig. 6c shows the optimal interaction strength for coherent particle hopping increasing with ξ, corroborating findings in Fig. 5. Except for very small ξ, U_{op} symbolizes the interaction strength from which coherent hopping becomes clearly predominant.

A notable behavior observed in Fig. 6 is the lack of non-coherent modes in the Fourier spectra as stronger interaction strengths are considered. Such behavior suggests a cooperative scenario consistent with the emergence of additional bound states. Indeed, long-range interaction gives rise to other bound states, as we report in Fig. 7. Here, we have applied a numerical diagonalization of the Hamiltonian (6) to an open chain with $N = 120$ sites in the absence of electric field and computed the normalized density of states (DOS) versus energy (E). Computational limitations have prevented us from reaching larger sizes. However, preliminary studies revealed no significant changes in DOS when exploring lattices with $N = 90$,100, and 110. We explored the increase in the U interaction strength and the ξ interaction range, considering $\xi = 0.5, 1.0, 2.0, 4.0$. For $\xi = 0.5$, we observe a sub-band emerging from the main band as the interparticle interaction U increases. This sub-band decouples around $U = 4$ and moves away from the main band as the interaction increases further. This behavior is consistent with characteristics reported in analytical [52] and numerical [25] studies for systems with solely on-site interactions, reinforcing previous findings for sufficiently small ξ values (Fig. 6). The emergence of distinct sub-bands of bound states is evident as we consider a more extended interaction range, such as $\xi = 1.0$. The first one matches with on-site bound states, while the latter is compatible with nearest-neighbor bound states. More bound states sub-bands emerge when considering an interaction range ξ even longer (see Fig. 7c–d). The third sub-band corresponds to bound states where particles occupy the next-nearest-neighbors, and so on. The emergence of these other sub-bands and the cooperative effect between the existing bound states are consistent with preserving coherent hopping for sufficiently strong interactions in Fig. 6. We observed the energy range of bound-states sub-bands varying as the interaction range ξ changes. As ξ increases, the sub-bands emerge from the main band for smaller interaction strengths, which corroborates the behavior of $\overline{\text{NOP}}$ in Fig. 5. Results also suggest a broadening of the on-site bound states sub-band as ξ increases, thus modifying the competitive scenario between bound and unbound states. Such behavior aligns with the increase in the optimal interaction for observing coherent hopping shown in Fig. 6, as well as the behavior of $\overline{\text{DOP}}$ in Fig. 5.

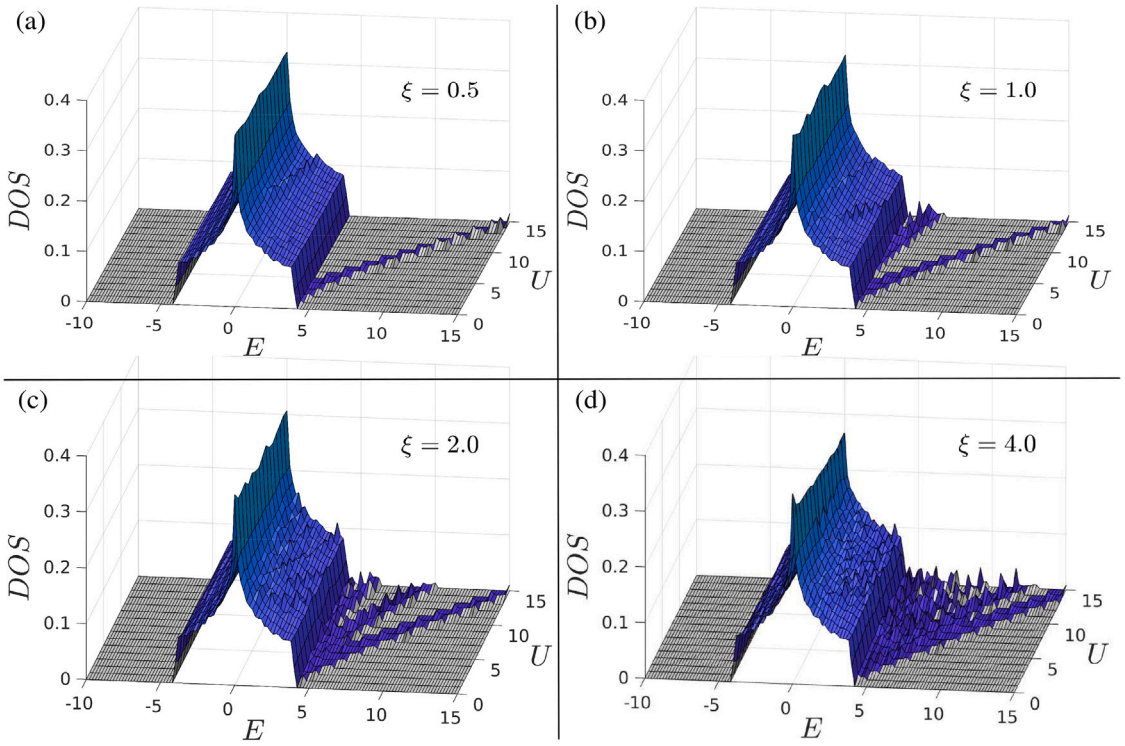

Fig. 7. The normalized density of states (DOS) versus energy (E) for distinct interaction strengths (U), by considering the interaction range (a) $\xi = 0.5$, (b) $\xi = 1.0$, (c) $\xi = 2.0$ and (d) $\xi = 4.0$. For ξ small enough, we observe the emergence of only a sub-band of bound states as U increases. This behavior is close to systems with particles exhibiting only on-site interaction. As the interaction range ξ increases, we observe the existence of other sub-bands of bound states, corroborating previous results regarding the cooperative effect of bound states.

4. Final remarks

In this work, we consider a system of interacting particles and study how the coexistence of local and non-local bound states influences particle dynamics. We explore two-particle quantum walking in tilted optical lattices, a framework with proven experimental viability and already-known dynamic signatures. We study systems with short- and long-range interactions between particles and observe the emergence of bound states directly associated with such interaction. Results show distinct correlated dynamics associated with dominant quantum states. On-site bound states from on-site interactions are responsible for correlated dynamics in which particles preferentially occupy the same site. Nearest-neighbor bound states lead to correlated dynamics in which particles preferentially occupy neighboring sites, and so on. The existing bound states are responsible for competitive and cooperative effects, which may give rise to unusual dynamics. We display the optimal scenarios for particles to perform coherent dynamics and how they change as a function of the interaction range. Thanks to the cooperative aspects between bound states, the nonmonotonic behavior exhibited by systems with only local interaction gives way to robustly correlated quantum walks, where coherent hopping is sustained even for strong interparticle interactions. As a result, our findings enhance comprehension of how available states in a quantum walk interplay with the underlying quantum correlations.

Beyond cold atoms trapped in optical lattices [22], which offer the versatility to combine multiple controls and measurements [43], photonic lattices [23,54], designed electric circuits [24], and superconducting processors [44,45] can map the dynamics of two interacting particles. This scenario positions them as promising frameworks for potential experimental investigations. To conclude, it would be interesting to have these results derived from an analytical framework, which would bring valuable new insights into the cooperative effects between bound states and quantum walks of particles hopping coherently.

CRediT authorship contribution statement

M.F.V. Oliveira: Writing – original draft, Methodology, Investigation, Data curation. **M.S. Santos Junior:** Writing – original draft, Methodology, Investigation, Data curation. **Michele B. Coêlho:** Writing – original draft, Methodology, Investigation, Data curation. **F.A.B.F. de Moura:** Writing – review & editing, Validation, Supervision, Methodology. **W.S. Dias:** Writing – review & editing, Validation, Supervision, Methodology, Investigation, Conceptualization.

Declaration of competing interest

The authors declare that they have no known competing financial interests or personal relationships that could have appeared to influence the work reported in this paper.

Data availability

Data will be made available on request.

Acknowledgments

This work was supported by CAPES (Coordenação de Aperfeiçoamento de Pessoal do Nível Superior), Brazil, CNPq (Conselho Nacional de Densenvolvimento Científico e Tecnológico), Brazil, and FAPEAL (Fundação de Apoio à Pesquisa do Estado de Alagoas), Brazil.

References

[1] R. Ionicioiu, P. Zanardi, Quantum-information processing in bosonic lattices, Phys. Rev. A 66 (2002) 050301.
[2] A.M. Childs, D. Gosset, Z. Webb, Universal computation by multiparticle quantum walk, Science 339 (6121) (2013) 791–794.
[3] R. Asaka, K. Sakai, R. Yahagi, Two-level quantum walkers on directed graphs. I. Universal quantum computing, Phys. Rev. A 107 (2023) 022415.
[4] A. Peruzzo, M. Lobino, J.C.F. Matthews, N. Matsuda, A. Politi, K. Poulios, X.-Q. Zhou, Y. Lahini, N. Ismail, K. Wörhoff, Y. Bromberg, Y. Silberberg, M.G. Thompson, J.L. OBrien, Quantum walks of correlated photons, Science 329 (5998) (2010) 1500–1503.
[5] J.K. Gamble, M. Friesen, D. Zhou, R. Joynt, S.N. Coppersmith, Two-particle quantum walks applied to the graph isomorphism problem, Phys. Rev. A 81 (2010) 052313.
[6] S.D. Berry, J.B. Wang, Two-particle quantum walks: Entanglement and graph isomorphism testing, Phys. Rev. A 83 (2011) 042317.
[7] D. Li, J. Zhang, F.-Z. Guo, W. Huang, Q.-Y. Wen, H. Chen, Discrete-time interacting quantum walks and quantum Hash schemes, Quantum Inf. Process. 12 (3) (2013) 1501–1513.
[8] M. Abraham, R. Berkovits, Persistent currents in an interacting 1D disordered ring: Manifestations of the Mott-Hubbard transition, Phys. Rev. Lett. 70 (1993) 1509–1512.
[9] A. Müller-Groeling, H.A. Weidenmüller, C.H. Lewenkopf, Interacting electrons in mesoscopic rings, Europhys. Lett. (EPL) 22 (3) (1993) 193–198.
[10] D.L. Shepelyansky, Coherent propagation of two interacting particles in a random potential, Phys. Rev. Lett. 73 (1994) 2607–2610.
[11] W. Dias, M. Lyra, Non monotonic influence of hubbard interaction on the Anderson localization of two-electron wavepackets, Physica A 411 (2014) 35–41.
[12] A. Peixoto, W. Dias, M. Lyra, F. de Moura, Wavepacket dynamics of coupled particles in aperiodic chains: Weakening of Anderson localization and local field effects, Physica A 395 (2014) 22–30.
[13] D. Semmler, K. Byczuk, W. Hofstetter, Mott-Hubbard and Anderson metal-insulator transitions in correlated lattice fermions with binary disorder, Phys. Rev. B 81 (2010) 115111.
[14] R. Vosk, E. Altman, Superfluid-insulator transition of ultracold bosons in disordered one-dimensional traps, Phys. Rev. B 85 (2012) 024531.
[15] Z. Ristivojevic, A. Petković, P. Le Doussal, T. Giamarchi, Phase transition of interacting disordered bosons in one dimension, Phys. Rev. Lett. 109 (2012) 026402.
[16] A. Habibi, E. Adibi, S.A. Jafari, Strong-coupling perturbative study of the disordered Hubbard model on the honeycomb lattice, Phys. Rev. B 98 (2018) 245105.
[17] E. Adibi, A. Habibi, S.A. Jafari, Phase transitions in the binary-alloy Hubbard model: Insights from strong-coupling perturbation theory, Phys. Rev. B 99 (2019) 014204.
[18] R.A. Vargas-Hernández, R.V. Krems, Quantum walks assisted by particle-number fluctuations, Phys. Rev. A 98 (2018) 022107.
[19] P. Rebentrost, M. Mohseni, I. Kassal, S. Lloyd, A. Aspuru-Guzik, Environment-assisted quantum transport, New J. Phys. 11 (3) (2009) 033003.
[20] J.P. Keating, N. Linden, J.C.F. Matthews, A. Winter, Localization and its consequences for quantum walk algorithms and quantum communication, Phys. Rev. A 76 (2007) 012315.
[21] L. Sansoni, F. Sciarrino, G. Vallone, P. Mataloni, A. Crespi, R. Ramponi, R. Osellame, Two-particle bosonic-Fermionic quantum walk via integrated photonics, Phys. Rev. Lett. 108 (2012) 010502.
[22] P.M. Preiss, R. Ma, M.E. Tai, A. Lukin, M. Rispoli, P. Zupancic, Y. Lahini, R. Islam, M. Greiner, Strongly correlated quantum walks in optical lattices, Science 347 (6227) (2015) 1229–1233.
[23] G. Corrielli, A. Crespi, G. Della Valle, S. Longhi, R. Osellame, Fractional Bloch oscillations in photonic lattices, Nature Commun. 4 (1) (2013) 1555.
[24] W. Zhang, H. Yuan, H. Wang, F. Di, N. Sun, X. Zheng, H. Sun, X. Zhang, Observation of Bloch oscillations dominated by effective anyonic particle statistics, Nature Commun. 13 (1) (2022) 2392.
[25] W.S. Dias, E.M. Nascimento, M.L. Lyra, F.A.B.F. de Moura, Frequency doubling of Bloch oscillations for interacting electrons in a static electric field, Phys. Rev. B 76 (2007) 155124.
[26] A. Ahlbrecht, A. Alberti, D. Meschede, V.B. Scholz, A.H. Werner, R.F. Werner, Molecular binding in interacting quantum walks, New J. Phys. 14 (7) (2012) 073050.
[27] A. Bisio, G.M. D'Ariano, P. Perinotti, A. Tosini, Thirring quantum cellular automaton, Phys. Rev. A 97 (2018) 032132.
[28] A. Bisio, G.M. D'Ariano, N. Mosco, P. Perinotti, A. Tosini, Solutions of a two-particle interacting quantum walk, Entropy 20 (6) (2018).
[29] R. Khomeriki, D.O. Krimer, M. Haque, S. Flach, Interaction-induced fractional Bloch and tunneling oscillations, Phys. Rev. A 81 (2010) 065601.
[30] X. Cai, H. Yang, H.-L. Shi, C. Lee, N. Andrei, X.-W. Guan, Multiparticle quantum walks and Fisher information in one-dimensional lattices, Phys. Rev. Lett. 127 (2021) 100406.
[31] M.K. Giri, S. Mondal, B.P. Das, T. Mishra, Signatures of nontrivial pairing in the quantum walk of two-component bosons, Phys. Rev. Lett. 129 (2022) 050601.
[32] S. Sarkar, T. Sowiński, Correlations in few two-component quantum walkers on a tilted lattice, Phys. Rev. A 102 (2020) 043326.
[33] C.H. Greene, P. Giannakeas, J. Pérez-Ríos, Universal few-body physics and cluster formation, Rev. Modern Phys. 89 (2017) 035006.
[34] M. Ganahl, E. Rabel, F.H.L. Essler, H.G. Evertz, Observation of complex bound states in the spin-1/2 heisenberg XXZ chain using local quantum quenches, Phys. Rev. Lett. 108 (2012) 077206.

[35] A. Morvan, T.I. Andersen, X. Mi, C. Neill, A. Petukhov, K. Kechedzhi, D.A. Abanin, A. Michailidis, R. Acharya, F. Arute, K. Arya, A. Asfaw, J. Atalaya, J.C. Bardin, J. Basso, A. Bengtsson, G. Bortoli, A. Bourassa, J. Bovaird, L. Brill, M. Broughton, B.B. Buckley, D.A. Buell, T. Burger, B. Burkett, N. Bushnell, Z. Chen, B. Chiaro, R. Collins, P. Conner, W. Courtney, A.L. Crook, B. Curtin, D.M. Debroy, A. Del Toro Barba, S. Demura, A. Dunsworth, D. Eppens, C. Erickson, L. Faoro, E. Farhi, R. Fatemi, L. Flores Burgos, E. Forati, A.G. Fowler, B. Foxen, W. Giang, C. Gidney, D. Gilboa, M. Giustina, A. Grajales Dau, J.A. Gross, S. Habegger, M.C. Hamilton, M.P. Harrigan, S.D. Harrington, M. Hoffmann, S. Hong, T. Huang, A. Huff, W.J. Huggins, S.V. Isakov, J. Iveland, E. Jeffrey, Z. Jiang, C. Jones, P. Juhas, D. Kafri, T. Khattar, M. Khezri, M. Kieferová, S. Kim, A.Y. Kitaev, P.V. Klimov, A.R. Klots, A.N. Korotkov, F. Kostritsa, J.M. Kreikebaum, D. Landhuis, P. Laptev, K.-M. Lau, L. Laws, J. Lee, K.W. Lee, B.J. Lester, A.T. Lill, W. Liu, A. Locharla, F. Malone, O. Martin, J.R. McClean, M. McEwen, B. Meurer Costa, K.C. Miao, M. Mohseni, S. Montazeri, E. Mount, W. Mruczkiewicz, O. Naaman, M. Neeley, A. Nersisyan, M. Newman, A. Nguyen, M. Nguyen, M.Y. Niu, T.E. O'Brien, R. Olenewa, A. Opremcak, R. Potter, C. Quintana, N.C. Rubin, N. Saei, D. Sank, K. Sankaragomathi, K.J. Satzinger, H.F. Schurkus, C. Schuster, M.J. Shearn, A. Shorter, V. Shvarts, J. Skruzny, W.C. Smith, D. Strain, G. Sterling, Y. Su, M. Szalay, A. Torres, G. Vidal, B. Villalonga, C. Vollgraff-Heidweiller, T. White, C. Xing, Z. Yao, P. Yeh, J. Yoo, A. Zalcman, Y. Zhang, N. Zhu, H. Neven, D. Bacon, J. Hilton, E. Lucero, R. Babbush, S. Boixo, A. Megrant, J. Kelly, Y. Chen, V. Smelyanskiy, I. Aleiner, L.B. Ioffe, P. Roushan, Formation of robust bound states of interacting microwave photons, Nature 612 (7939) (2022) 240–245.
[36] S.-J. Gu, S.-S. Deng, Y.-Q. Li, H.-Q. Lin, Entanglement and quantum phase transition in the extended hubbard model, Phys. Rev. Lett. 93 (2004) 086402.
[37] J. Kempe, Quantum random walks: An introductory overview, Contemp. Phys. 44 (4) (2003) 307–327.
[38] O. Mülken, A. Blumen, Continuous-time quantum walks: Models for coherent transport on complex networks, Phys. Rep. 502 (2) (2011) 37–87.
[39] S.E. Venegas-Andraca, Quantum walks: a comprehensive review, Quantum Inf. Process. 11 (5) (2012) 1015–1106.
[40] M. Gong, S. Wang, C. Zha, M.-C. Chen, H.-L. Huang, Y. Wu, Q. Zhu, Y. Zhao, S. Li, S. Guo, H. Qian, Y. Ye, F. Chen, C. Ying, J. Yu, D. Fan, D. Wu, H. Su, H. Deng, H. Rong, K. Zhang, S. Cao, J. Lin, Y. Xu, L. Sun, C. Guo, N. Li, F. Liang, V.M. Bastidas, K. Nemoto, W.J. Munro, Y.-H. Huo, C.-Y. Lu, C.-Z. Peng, X. Zhu, J.-W. Pan, Quantum walks on a programmable two-dimensional 62-qubit superconducting processor, Science 372 (6545) (2021) 948–952.
[41] Y. Aharonov, L. Davidovich, N. Zagury, Quantum random walks, Phys. Rev. A 48 (1993) 1687–1690.
[42] E. Farhi, S. Gutmann, Quantum computation and decision trees, Phys. Rev. A 58 (1998) 915–928.
[43] F. Schäfer, T. Fukuhara, S. Sugawa, Y. Takasu, Y. Takahashi, Tools for quantum simulation with ultracold atoms in optical lattices, Nat. Rev. Phys. 2 (8) (2020) 411–425.
[44] Z. Yan, Y.-R. Zhang, M. Gong, Y. Wu, Y. Zheng, S. Li, C. Wang, F. Liang, J. Lin, Y. Xu, C. Guo, L. Sun, C.-Z. Peng, K. Xia, H. Deng, H. Rong, J.Q. You, F. Nori, H. Fan, X. Zhu, J.-W. Pan, Strongly correlated quantum walks with a 12-qubit superconducting processor, Science 364 (6442) (2019) 753–756.
[45] Y. Ye, Z.-Y. Ge, Y. Wu, S. Wang, M. Gong, Y.-R. Zhang, Q. Zhu, R. Yang, S. Li, F. Liang, J. Lin, Y. Xu, C. Guo, L. Sun, C. Cheng, N. Ma, Z.Y. Meng, H. Deng, H. Rong, C.-Y. Lu, C.-Z. Peng, H. Fan, X. Zhu, J.-W. Pan, Propagation and localization of collective excitations on a 24-qubit superconducting processor, Phys. Rev. Lett. 123 (2019) 050502.
[46] R. Morandotti, U. Peschel, J.S. Aitchison, H.S. Eisenberg, Y. Silberberg, Experimental observation of linear and nonlinear optical Bloch oscillations, Phys. Rev. Lett. 83 (1999) 4756–4759.
[47] F. Domínguez-Adame, Beyond the semiclassical description of Bloch oscillations, Eur. J. Phys. 31 (3) (2010) 639.
[48] D. Bohm, D. Pines, A collective description of electron interactions: III. Coulomb interactions in a degenerate electron gas, Phys. Rev. 92 (1953) 609–625.
[49] F. Bloch, Über die Quantenmechanik der Elektronen in Kristallgittern, Z. Phys. 52 (7) (1929) 555–600.
[50] D.H. Dunlap, V.M. Kenkre, Dynamic localization of a charged particle moving under the influence of an electric field, Phys. Rev. B 34 (1986) 3625–3633.
[51] A. Peixoto, W. Dias, The role of on-site and nearest-neighbor interactions in the correlated two-particles quantum walk, Solid State Commun. 242 (2016) 68–73.
[52] J. Hubbard, B.H. Flowers, Electron correlations in narrow energy bands, Proc. R. Soc. Lond. Ser. A. 276 (1365) (1963) 238–257.
[53] H. Sun, B. Yang, H.-Y. Wang, Z.-Y. Zhou, G.-X. Su, H.-N. Dai, Z.-S. Yuan, J.-W. Pan, Realization of a bosonic antiferromagnet, Nat. Phys. 17 (9) (2021) 990–994.
[54] S. Longhi, Photonic Bloch oscillations of correlated particles, Opt. Lett. 36 (16) (2011) 3248–3250.